Accepted Manuscript

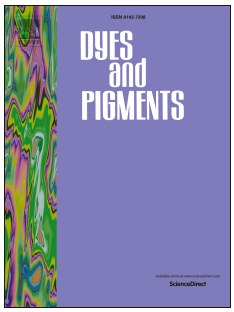

Synthesis and characterization of highly soluble phenanthro[1,10,9,8-*c*,*d*,*e*,*f*,*g*]carbazole-based copolymer: Effects of thermal treatment on crystalline order and charge carrier mobility

Nam Yeong Jeong, Min Su Jang, So Min Park, Dae Sung Chung, Yun-Hi Kim, Soon-Ki Kwon

PII: S0143-7208(17)31957-5

DOI: 10.1016/j.dyepig.2017.10.044

Reference: DYPI 6343

To appear in: *Dyes and Pigments*

Received Date: 14 September 2017

Revised Date: 30 October 2017

Accepted Date: 30 October 2017

Please cite this article as: Jeong NY, Jang MS, Park SM, Chung DS, Kim Y-H, Kwon S-K, Synthesis and characterization of highly soluble phenanthro[1,10,9,8-*c*,*d*,*e*,*f*,*g*]carbazole-based copolymer: Effects of thermal treatment on crystalline order and charge carrier mobility, *Dyes and Pigments* (2017), doi: 10.1016/j.dyepig.2017.10.044.

Synthesis and characterization of highly soluble Phenanthro[1,10,9,8-c,d,e,f,g]carbazole-based copolymer: effects of thermal treatment on crystalline order and charge carrier mobility

Nam Yeong Jeong†[1], Min Su Jang†[3], So Min Park[2], Dae Sung Chung[3]*, Yun-Hi Kim[1]*, Soon-Ki Kwon[2]*

[1]*Department of Chemistry and RINS, Gyeongsang National University, Jinju 660-701 Korea,*

[2]*Department of Materials Engineering and Convergence Technology and ERI, Gyeongsang National University, Jinju 660-701, Korea*

[3]*Department of Energy Systems Engineering, Daegu Gyeongbuk Institute of Science and Technology (DGIST), Daegu 42988, Republic of Korea*

†These authors contributed equally to this work.

Abstract

In this study, a novel donor-acceptor type semiconducting polymer was designed and synthesized based on phenanthro[1,10,9,8-c,d,e,f,g]carbazole backbone. The resulting polymer, poly[4-(5-(6-(2-decyltetradecyl)-6*H*-phenanthro[1,10,9,8-c,d,e,f,g]carbazol-4-yl)thiophen-2-yl)-5,6-bis(octyloxy)-7-(thiophen-2-yl)benzo[*c*][1,2,5]thiadiazole] (PPTBTT), exhibited high solubility in various solvents which enables facile fabrication of semiconducting devices such as thin-film transistors, and also opens up possibilities for large scale solution processing. Absorption spectra of PPTBTT showed large bathochromic shift when the polymer was prepared as a thin-film, which can be explained by the high solubility and molecular packing of the synthesized polymer. X-ray diffraction measurements showed that the crystalline structure of PPTBTT polymer film is largely influenced by the thermal treatment temperature. Together with the atomic force microscopy data, it was found that the

optimal thermal treatment temperature of PPTBTT film is 170 °C. The charge transfer characteristics were confirmed by fabricating PPTBTT thin-film transistor. In accordance with the polycrystalline structure, PPTBTT film transistor showed the highest mobility of 0.0092 $cm^2 V^{-1} s^{-1}$ and on/off ratio of 10^4 when the device was annealed at 170 °C.

KEYWORDS

phenanthrocarbazole; high solubility; annealing; thin films; organic field effect transistor

1. Introduction

Organic semiconducting polymers have gained significant attention for decades for their unique characteristics such as solution processability, flexibility, and cost-efficient device fabrication.[1-4] Utilizing these advantages, organic optoelectronic devices such as organic field effect transistors (OFETs), organic photovoltaic cells (OPVs), and organic light emitting diodes (OLEDs) have achieved high performances by optimizing and developing polymers that best suit each device.[5-8] One of the most important considerations in polymer design is choosing the right building block for the polymer. Among many, carbazole derivatives are considered very effective building blocks due to their π-extended fused rings that ensure planarity and electron delocalization along the polymer backbone.[9-10] This coplanar backbone enables intermolecular π overlap, which opens up possibilities for effective charge transport characteristics and intermolecular interactions with neighboring polymer chains, leading to a high charge carrier mobility for the fabricated device.[11] The carbazole unit also has a great advantage in that it can be easily tuned at various sites. By attaching various molecules to the carbazole building block, the various the characteristics of the resulting polymer can be optimized for the device application.[12] However, a lot of these approaches

are aimed at extending the effective conjugation length along the horizontal direction of the polymer main chain.[13-19] Reports on ladder-type building blocks with extended π-conjugation along the vertical direction of the polymer main chain are relatively scarce,[20-21] even though such reports have shown polymers with notable results when applied to devices such as OFET, OPV, and organic photodiodes (OPD).[22-24] Thus, further research on such vertically extended carbazole derivatives could show great potential for developing novel organic semiconducting polymers.

Herein, we report a semiconducting polymer with 6*H*-phenanthro[1,10,9,8-c,d,e,f,g]carbazole (PCZ) as the building block. The PCZ building block, which has a ladder type π-extended fused aromatic ring underneath the carbazole structure, utilized all the aforementioned benefits of the carbazole unit. Additionally, the polyacene system underneath the carbazole core increased the effective conjugation length of the polymer and also contributed to the planarity of the polymer backbone. Furthermore, the electron rich amine functional group on the PCZ molecule ensured electron donating capability, making it a suitable candidate for the donor moiety in a donor-acceptor (D-A) configuration. For the acceptor moiety, 4,7-bis(3,4-bis(octyloxy)thiophen-2-yl)benzo[*c*][1,2,5]thiadiazole was chosen to further maximize the characteristics of the PCZ backbone. The planar structure of the acceptor unit could further contribute to the planarity of the building block while the electron deficient benzothiadiazole effectively reduced the electron density, which induced a broad light absorption spectrum.[25] Due to the high coplanarity of both the donor and acceptor moiety, the resulting polymer, poly[4-(5-(6-(2-decyltetradecyl)-6*H*-phenanthro[1,10,9,8-c,d,e,f,g]carbazol-4-yl)thiophen-2-yl)-5,6-bis(octyloxy)-7-(thiophen-2yl)benzo[*c*][1,2,5]thiadiazole] (PPTBTT), would benefit from strong intermolecular

interactions with nearby polymer chains, which would be advantageous for effective charge transport, and would form a compact film structure. However, the strong interchain interaction induced by the polyaromatic conjugated structure is known to make polymers insoluble in solvents, which limits its processability. Thus, long alkyl and alkoxy chains were employed on the donor and acceptor moieties, respectively, to ensure high solubility in various solvents. To confirm its high solution processability and charge transport characteristics, we fabricated an OFET device that formed a compact film from a simple spin coating technique and that exhibited a hole mobility of 0.009 $cm^2 V^{-1} s^{-1}$ with a current on/off ratio of 10^4.

2. Experimental

2.1 Materials

2,1,3-Benzothiadiazole, bromine, sodium borohydride, dimethylformamide (DMF), tetrakis(triphenylphosphine)palladium and all solutions were purchased from Aldrich. All chemicals were used without further purification.

2.2 Synthesis

6-(2-Decyltetradecyl)-4,8-bis(4,4,5,5-tetramethyl-1,3,2-dioxaborolan-2-yl)-6*H*-phenanthro[1,10,9,8-c,d,e,f,g]carbazole (1) The synthesis followed reported methods.[21, 22, 24] The crude product was purified by chromatography using petroleum ether/dichloromethane (3:1) to obtain a yellow solid. Yield: 1.28 g (32%). mp: 165 °C. ^{1}H-NMR ($CDCl_3$): 9.01-8.98 (d, J=9Hz. 2H), 8.74-8.72 (d, J=7.4Hz 2H), 8.50 (s, 2H), 7.92-7.86 (m, 2H), 4.72 (d, J=7.4Hz, 2H), 2.34 (m, 1H), 1.52 (s, 24H), 1.43-1.39 (m, 6H), 1.21 (m, 34H), 0.90-0.86 (m, 6H). ^{13}C-NMR ($CDCl_3$): 133.23, 132.71, 132.69, 132.66, 131.50, 130.99,

125.33, 125.25, 125.15, 125.12, 124.53, 123.15, 122.68, 121.12, 120.89, 120.56, 120.16, 84.00, 50.18, 40.14, 34.75, 32.18, 32.15, 32.07, 30.30, 30.06, 30.01, 29.98, 29.73, 26.85, 26.79, 25.47, 23.32, 23.05, 14.49.

4,7-Bis(5-bromothiophen-2-yl)-5,6-bis(octyloxy)benzo-[C][1,2,5]-thiadiazole (2) A mixture of 5,6-bis(octyloxy)-4,7-di(thiophen-2-yl)benzo[*c*][1,2,5]thiadiazole (2.56 g, 4.6 mmol), *N*-bromosuccinimide (NBS) (1.83 g, 10.2 mmol), glacial acetic acid (100 mL), and chloroform (100 mL) was reacted at room temperature in dark condition for 24 h. The solvent was removed under reduced pressure, and the crude compound was purified by chromatographically methylene chloride/hexane (1:10) as eluent to give the product as an orange crystal. Yield: 2.56 g (78%). mp: 77 °C. ^{1}H NMR ($CDCl_3$): 8.37–8.36 (d, J=4.1Hz 2H), 7.18–7.16 (d, J=4.3Hz 2H), 4.12–4.10 (t, J=7.2Hz, 4H), 1.97–1.90 (m, 4H), 1.47–1.25 (m, 20H), 0.91–0.87 (m, 6H). ^{13}C-NMR ($CDCl_3$): 151.52, 150.43, 135.71, 131.02, 129.70, 117.02, 115.47, 74.60, 31.83, 30.28, 29.47, 29.29, 25.93, 22.69, 14.13. MS (EI) m/z: 714 (M+).

Poly[4-(5-(6-(2-decyltetradecyl)-6*H*-phenanthro[1,10,9,8-c,d,e,f,g]carbazol-4-yl)thiophen-2-yl)-5,6-bis(octyloxy)-7-(thiophen-2-yl)benzo[*c*][1,2,5]thiadiazole] (PPTBTT) The polymer was synthesized by Suzuki coupling reaction. All handling of catalysts and polymerization were carried out in a nitrogen atmosphere. 4,7-Bis(5-bromothiophen-2-yl)-5,6-bis(octyloxy)benzo[*c*][1,2,5]thiadiazole (0.3 g, 0.4 mmol) in toluene (7 mL), a 2 M K_2CO_3 solution (1.41 mL) in water, and $Pd(PPh_3)_4$ (0.01 g, 0.5 mol%) were added to a stirred solution of 6-(2-decyltetradecyl)-4,8-bis(4,4,5,5-tetramethyl-1,3,2-dioxaborolan-2-yl)-6*H*-phenanthro[1,10,9,8-c,d,e,f,g]carbazole (0.4 g, 0.4 mmol). The polymerization was carried out at 95 °C for 72 h. The end-capping reaction was done by 2-

bromobenzene (0.1 g, 4.8 mmol). The crude polymer was dissolved in $CHCl_3$ and was precipitated in methanol. The polymer was purified successive Soxhlet. Yield: 61%. ^{1}H NMR ($CDCl_3$) (ppm): 8.70 (br, 4H), 8.62-8.60 (br, 2H), 8.01 (br, 2H), 7.86-7.83 (br, 2H), 7.58 (br, 2H) 4.60-4.56 (br, 2H), 4.22-4.20 (br, 4H), 2.02 (br, 4H), 1.47-1.02 (br, 57H), 0.88 (br, 12H). IR FT-IR (KBr) (cm^{-1}): 3052 (aromatic), 2926 (aliphatic, C-H), 1650 (aromatic, C=C), 1440 (aromatic, C-C), 812 (aromatic, C-S). The number average molecular weight (Mw) : 27.3 kg mol^{-1} , PDI : 1.34.

2.3 OFET Device Fabrication and Characterization

A Silicon wafer with a 100-nm thick SiO_2 dielectric layer on heavily n-doped silicon was used as the substrate. The substrate was cleaned in a piranha solution. The semiconducting polymer, poly [4-(5-(6-(2-decyltetradecyl)-6*H*-phenanthro[1,10,9,8-c,d,e,f,g]carbazol-4-yl)thiophen-2-yl)-5,6-bis(octyloxy)-7-(thiophen-2-yl)benzo[*c*][1,2,5]thiadiazole] (**PPTBTT**) (5 mg), was dissolved in an anhydrous chloroform solution (1 mL). An octyltrichlorosilane (OTS)-modified SiO_2 surface was prepared by immersing the substrate in OTS (0.3 mL) in toluene (60 mL) at 40 °C for 30 min, followed by thermal annealing at 120 °C for 30 min. The PPTBTT solution was spin-coated onto the OTS-modified substrate at 2000 rpm for 30 s and then annealed at temperatures of 25, 150, 170, and 200 °C. The source-drain electrodes were deposited on top of an annealed PPTBTT film to complete the top-contact/bottom-gate architecture. The electrical characteristics of the transistors were measured by an HP4156A Precision semiconductor parameter analyzers (Agilent Technologies) and LabView-controlled Keithley 2400 source measure unit.

2.4 Measurements

^{1}H NMR spectra were recorded with Bruker Advance-300 and 500 spectrometers, and IR

spectra were measured by a Varian 640-IR FTIR spectrometer. Thermogravimetric analysis (TGA) was performed on a TA Instruments TGA 2100 in a nitrogen atmosphere at a rate of 10 °C/min, and differential scanning calorimetry (DSC) was conducted under nitrogen on a TA Instruments 2100 DSC with a heating rate of 10 °C/min from 30 °C to 300 °C. Molecular weights and polydispersity indices (PDIs) of the copolymers were determined by gel permeation chromatography (GPC) analysis with a polystyrene standard calibration (Waters high-pressure GPC assembly, Model M515 pump, u-Styragel HR4, HR4E, and HR5E columns, 500 and 100 Å resolution, refractive index detectors, solvent THF). Cyclic voltammetry (CV) was performed on an EG&G Parc model 273A potentiostat/galvanostat system with a three-electrode cell in a solution of tetrabutylammonium perchlorate (Bu_4NClO_4) (0.1 mol) in acetonitrile at a scan rate of 50 mV/s. The polymer films were coated on a square carbon electrode by dipping the electrode into the corresponding solvents and then were dried under nitrogen. A Pt wire was used as the counter electrode, and an $Ag/AgNO_3$ (0.1 mol) electrode was used as the reference electrode. UV–vis absorption spectra were measured by a UV-1650PC spectrophotometer (Shimadzu). Grazing incident X-ray diffraction (GIXD) measurements were performed using the PLS-II 3C, 9A U-SAXS beamline at the Pohang Accelerator Laboratory (PAL) in Korea. The X-rays coming from the in-vacuum undulator (IVU) were monochromatized (E = 11.06 keV) using Si (111) double crystals and then focused at the detector position by using a K−B focusing mirror system. The horizontal and vertical beam sizes were 300 (*H*) μm and 30 (V) μm, respectively. The incidence angle (α_i) was adjusted to 0.13°, which is above the critical angle. GIXD patterns were recorded with a 2D CCD detector (Rayonix, SX-165). The diffraction angles were calibrated using precalibrated sucrose (Monoclinic, P21), and the sample-to-detector distance was approximately 225 mm. All the morphological images were obtained using an atomic

force microscope (AFM, Park systems, XE7)

3. Results and Discussion

3.1 Synthesis

The synthetic route for preparing the polymer is shown in Scheme 1. The crude PPTBTT was purified by successive Soxhlet extractions to remove byproducts and oligomers. The chemical structures of the monomers and polymer were verified through ^{1}H NMR, ^{13}C NMR, and mass spectrometry (Figure S1 and Figure S2). The synthesized polymer showed good solubility in common organic solvents such as THF, toluene, chloroform, chlorobenzene (CB), and dichlorobenzene (DCB), due to the bulky alkyl chain and alkoxy side chains. Such high solubility of PPTBTT in various solvents opens the possibility to use a solution process with an environmentally benign solvent for organic electronic devices such as OFET and OPV. The molecular weight of the polymer was determined by using GPC against polystyrene standards in THF. The number average molecular weight (Mw) of PPTBTT is 27.3 kg mol^{-1} with a corresponding PDI of 1.34, respectively. The TGA and DSC analysis of the polymer suggests good thermal stability, showing less than 5% weight loss at temperatures up to 336°C. (Figure S3) Considering that the T_g of the polymer is between 150°C and 200°C, the polymer film was analyzed within this temperature range.

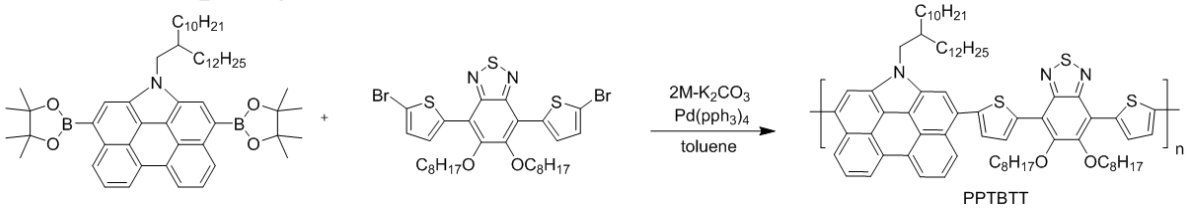

Scheme 1. Synthetic routes of the PPTBTT copolymer

3.2 Optical Properties

The normalized UV-vis absorption spectra of synthesized PPTBTT in a dilute solution state and thin film state are shown in Figure 1. The absorption spectrum of PPTBTT in chloroform solution showed a maximum absorption peak at 530 nm (ε =40,000 $M^{-1}cm^{-1}$), while the absorption spectrum in the film state showed a maximum absorption peak at 573 nm. Both had a wide absorption spectrum due to the strong interaction between the electron rich donor and electron deficient acceptor. Noticeably, the absorption spectrum between the solution and film states shows a remarkable bathochromic shift of about 43 nm. This large discrepancy between the two absorption peaks implies that the synthesized PPTBTT would have high solubility in chloroform solution, with the polymer molecules freely dispersed within the solution due to the long side chains.

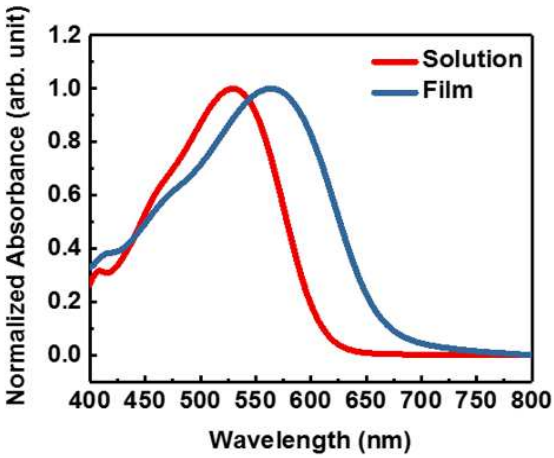

Figure 1. Absorption spectra of PPTBTT in $CHCl_3$ solution and as thin film

In the solution state, the strong intermolecular interaction induced by the planar polyaromatic backbone was largely reduced by the steric hindrance imparted by the long side chains, which

increased the disorder of the conjugated system and the interchain distance.[26] In addition, when spin-coated onto the glass substrate, the PPTBTT film exhibited high molecular packing. When prepared as a thin-film, the interchain distance became closer, and the intermolecular interactions became stronger due to the planar backbone design of PPTBTT. These results are consistent with the goal of designing a solution processable polymer that can form a compact solid film with a simple approach such as spin coating.

3.3 Structure of Polymer Thin Films

To better understand the structural charL13-acteristics of PPTBTT in the film state, two-dimensional GIXD (2D-GIXD) analysis was conducted to investigate the crystalline orientation. To observe the change in intermolecular crystalline order, GIXADS analyses were conducted on PPTBTT films annealed at different temperatures (25, 150, 170, and 200 °C). The out-of-plane line cuts are summarized in Figure S4. As shown in the diffraction patterns (Figure 2), an amorphous halo in the q = 0.17~0.21 $Å^{-1}$ range is visible for films without any thermal treatment. This amorphous halo implies that the large portion of bulk PPTBTT backbone (> 30 Å) had an amorphous orientation without thermal annealing. With increasing temperature, this amorphous halo faded out and could no longer be clearly observed in films annealed at 150 °C. Noticeably, a clear (001) peak, which shows the ordering along the polymer backbone, is visible at q = 0.22 $Å^{-1}$ once the film reached 150 °C. As such, the spacing between polymer backbones became closely packed, and the polymers thus formed a compact molecular structure. Surprisingly, the PPTBTT films annealed at 170 °C showed a long range ordered structure with much more defined out-of-plane Bragg diffraction peaks up to (005). However, upon reaching an annealing temperature of 200 °C, the out-of-plane oriented peaks diminished, implying lower crystalline structure.

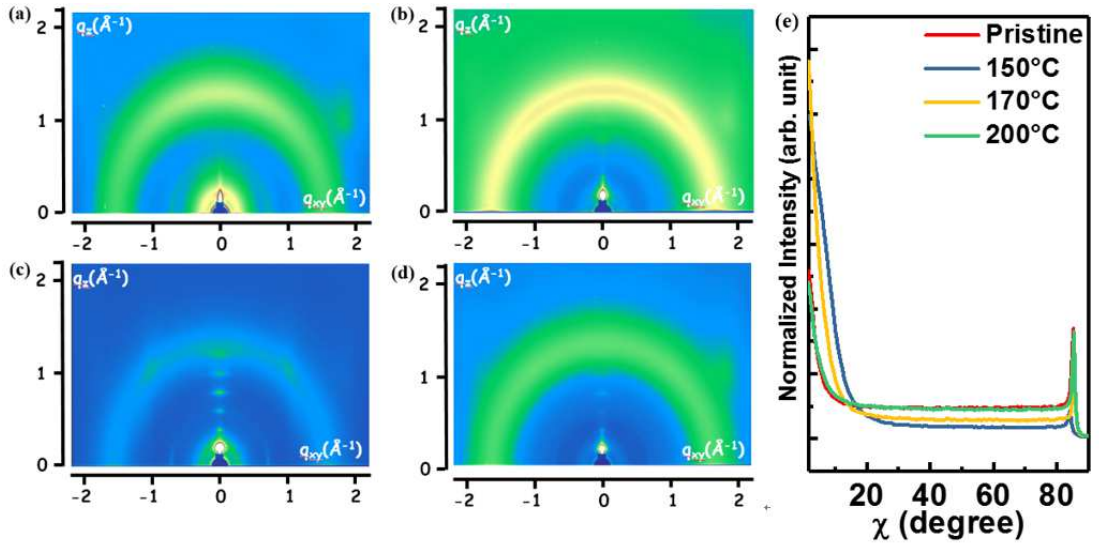

Figure 2. GIXD patterns of PPBTT films annealed at (a) 25 °C, (b) 100 °C, (c) 150 °C, and (d) 170 °C for 10 minutes. Pole figures of PPTBTT films annealed at different temperatures are summarized in (e).

Thus, 170 °C was found to be the optimal temperature for PPTBTT molecules to form a highly crystalline structure, which plays a crucial role in charge transport. Additionally, the pole figure analysis of the PPTBTT film (Figure 2e) shows a stronger edge-on crystal orientation with increasing temperature up to 170 °C. Such orientation is well known to have superior charge transport characteristics in a lateral-type device.

3.4 Thin Film Microstructure

To further analyze the structural characteristics of the PPTBTT film, atomic force microscopy (AFM) measurements were carried out to investigate the change in film morphology upon annealing. Samples were prepared in accordance with the GIXD samples. As shown in Figure 3, PPTBTT films without thermal treatment show featureless film

morphology with a very low root-mean-square (rms) roughness of 0.8 nm. However, the AFM image of PPTBTT film annealed at 150 °C shows an increase in crystallinity with polycrystalline grains emerging from the previously featureless film. Even larger polycrystalline grains were formed when the annealing temperature increased to 170 °C. The increase in polycrystalline grains and their interconnectivity would ensure effective charge transport in the film state. Similar to the GIXD results, the clearly visible polycrystalline grains became vague and once again showed a featureless film morphology once the film was annealed at 200 °C. The AFM image and the GIXD data of the PPTBTT film suggested that the annealing temperature significantly affected the crystalline order and morphology of the PPTBTT film, showing the most favorable film state at 170 °C for effective charge transfer. Above 200 °C, the crystal structure of the PPTBTT film seemed to collapse due to thermal stress.

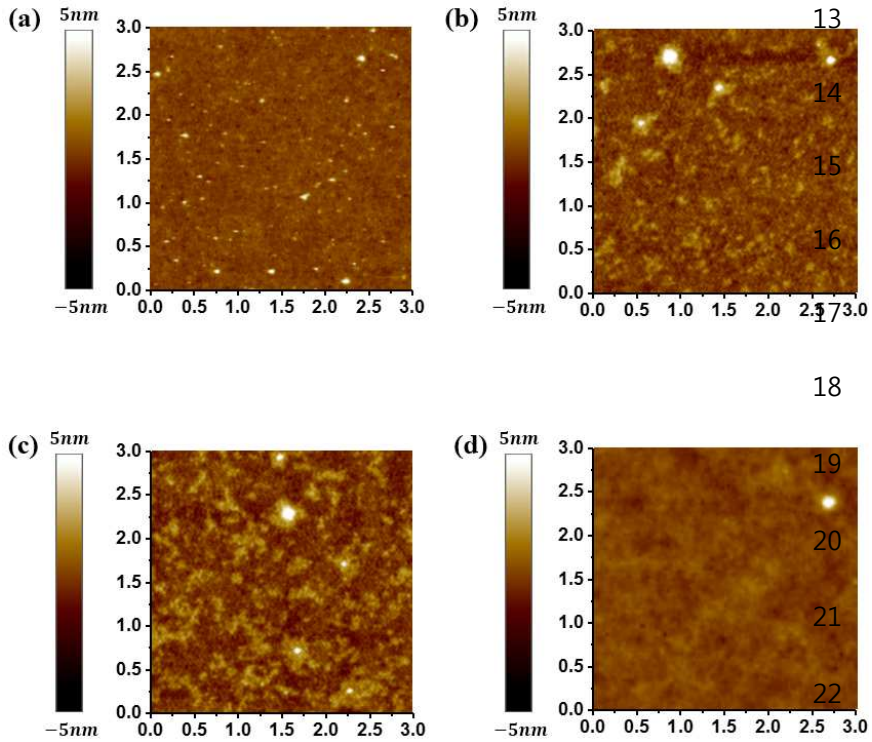

Figure 3. AFM images of PPTBTT film surface on the OTS-modified SiO_2/Si substrates annealed at (a) 25 °C, (b) 150 °C, (c) 170 °C, and (d) 200 °C for 10 minutes.

3.5 Field-Effect Transistors Characteristics

To confirm the charge transport characteristics of the solution processed PPTBTT films, top-contact-electrode OFETs (L=150 μm and W=1500 μm) were fabricated. Figure 4 shows drain current-gate voltage (*ID - VG*) transfer curves of the OFETs with PPTBTT films annealed at different temperatures, operated at the saturation regime (drain voltage V_D= -30 V). Table 1 summarizes the electrical properties of the fabricated OFETs. All the fabricated devices showed typical p-type transistor behavior with output curves showing excellent saturation behavior. Noticeably, the electrical performance of the fabricated devices showed improvement with temperature up to 170 °C, consistent with the previous data in the GIXD and AFM measurements. With increasing temperature, the highly π-conjugated PPTBTT polymer showed self-assembling characteristics, forming a closely packed molecular structure. Such molecular structure enabled strong intermolecular interactions, greatly enhancing the charge transport characteristics. Without any thermal annealing, the field-effect mobility (μ_{FET}) of the OFET fabricated from pristine PPTBTT films showed a low value of 0.0018 cm^2 V^{-1} s^{-1} due to the highly amorphous molecular structure with no significant polycrystalline structure.

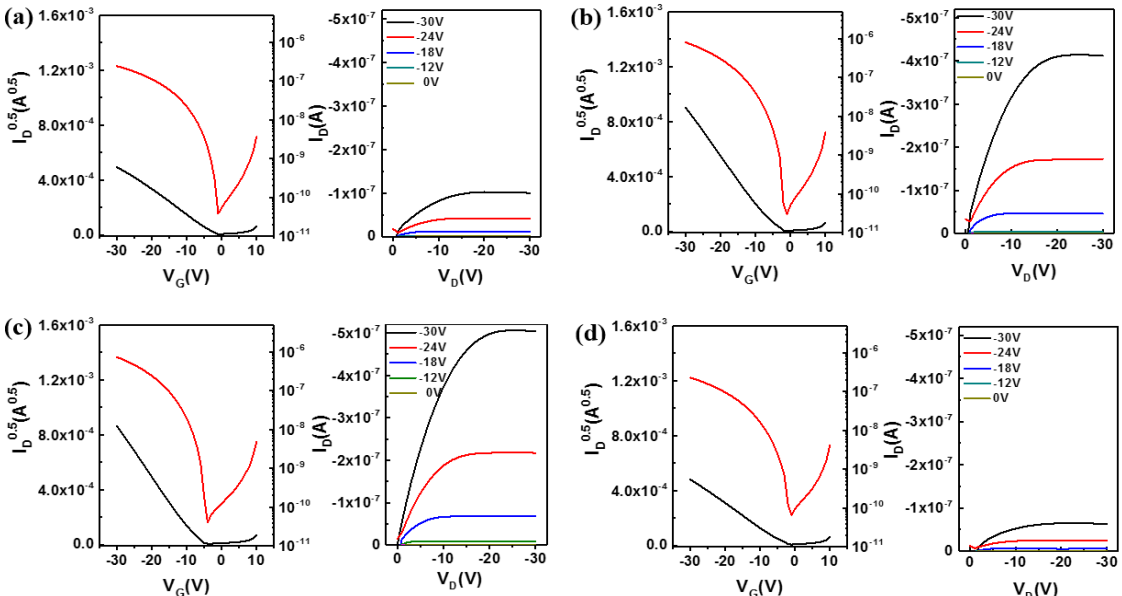

Figure 4. Transfer (left) and output (right) characteristics of PPTBTT film based devices annealed at 25 °C, 150 °C, 170 °C, and 200 °C.

Table 1. Field-Effect Characteristics for PPTBTT films based on different annealing temperatures

	Annealing Temperature	Mobility ($^{cm^2}/_{Vs}$)	on/off	V_{th} (V)
PPTBTT	Pristine	0.0018 (Ave.) 0.0020 (Max.)	10^3	-1
	150°C	0.0079 (Ave.) 0.0081 (Max.)	10^4	-1
	170°C	0.0085 (Ave.) 0.0092 (Max.)	10^4	-4
	200°C	0.0020 (Ave.) 0.0021 (Max.)	10^3	-1

However, OFET fabricated from PPTBTT film annealed at 170 °C showed a maximum μ_{FET} up to 0.0092 cm^2 V^{-1} s^{-1}, a substantial increase from the μ_{FET} of the pristine PPTBTT film OFET. Thermal annealing exceeding 200 °C showed poor electrical properties due to the poor crystalline structure and featureless film morphology.

4. Conclusion

In summary, a novel donor-acceptor type semiconducting polymer with highly planar PCZ units was designed and synthesized by the common Suzuki-coupling reaction. The synthesized polymer showed excellent solubility in various solvents due to the long side chains on both the donor and acceptor moieties, which opens the possibility for various solution process techniques such as spin-coating, spray coating, and bar coating. UV-vis spectra measurement confirmed the high solubility of the PPTBTT polymer and showed high

molecular packing in the film state. The 2D-GIXD and AFM results suggested that thermal annealing (at 170 °C for 10 min) induced large polycrystalline grains that showed long range ordered structure with a highly edge-on orientation. All these characteristics are favorable for charge transport. When fabricated into an OFET, the PPTBTT film without any thermal annealing showed a field-effect mobility (μ_{FET}) of 0.0018 cm^2 V^{-1} s^{-1}, while the film annealed at 170 °C showed a surprising enhancement in μ_{FET} up to 0.0092 cm^2 V^{-1} s^{-1}. The increase in field-effect mobility can be attributed to the high intermolecular interactions induced by the favorable structural order of the polymer film mentioned above. The solution processability, electrical properties, and relatively simple synthesis of PPTBTT fulfill well the requirements for applications in large scale solution printing of cost-efficient OFET arrays.

Acknowledgements

This research was financially supported by the National Research Foundation of Korea (NRF) funded by Korea government (MSIP) (2015R1A2A1A10055620, NRF-2014M1A3A3A02034707, and 2016M1A2A2940911).

References

[1] V. L. Colvin, M. C. Schlamp, and A. P. Alivisatos, *Nature* **1994**, 370, 354.
[2] McCulloch, M. Heeney, C. Bailey, K. Genevicius, I. MacDonald, M. Shkunov, D. Sparrowe, S. Tierney, R. Wagner, and W. Zhang, *Nat. Mater.* **2006**, 5(4), 328.
[3] D. Braun, and A. J. Heeger, *Appl. Phys. Lett.* **1991**, 58(18), 1982.
[4] C. Jiao, K. W. Huang, Z. Guan, Q. H. Xu, and J. Wu, *Org. Lett.* **2010**, 12(18), 4046.
[5] K. Gunasekar, W. Cho, D. X. Long, S. S. Reddy, M. Song, Y. Y. Noh, and S. H. Jin, *Adv. Electron. Mater.* **2016**, 2(8), 1600086.
[6] L. Ren, H. Fan, D. Huang, D. Yuan, C. A. Di, and X. Zhu, *Chem.-Eur. J.* **2016**, 22(48), 17136.
[7] A. Tang, C. Zhan, J. Yao, and E. Zhou, *Adv. Mater.* **2016**, 29(2), 1600013.

[8] C. Zhan, and J. Yao, *Chem. Mat.* **2016,** 28(7), 1948.
[9] A. Venkateswararao, K. R. J. Thomas, C. P. Lee, C. T. Li, and K. C. Ho, *ACS Appl. Mater. Interfaces* **2014**, 6(4), 2528.
[10] Q. Zhang, J. Li, K. Shizu, S. Huang, S. Hirate, H. Miyazaki, and C. Adachi, *J. Am. Chem. Soc.* **2012**, 134(36), 14706.
[11] Y. Wu, Y. Li, S. Gardner, and B. S. Ong, J. *Am. Chem. Soc.* **2005**, 127(2), 614.
[12] H. Wang, F. Liu, L. H. Xie, C. Tang, B. Peng, W. Huang, and W. Wei, *J. Phys. Chem. C.* **2011**, 115(14), 6961.
[13] F. Lyu, H. Park, S. H. Lee, S. H. Lee, and Y. S. Lee, *Chem. Phys. Lett.* 2014, **610,** 388.
[14] P. C. Jwo, Y. Y. Lai, C. E. Tsai, Y. Y. Lai, W. W. Liang, C. S. Hsu, and Y. J. Cheng, *Macromolecules* **2014**, 47(21), 7386.
[15] J. S. Wu, Y. J. Cheng, T. Y. Lin, C. Y. Chang, P. I. Shih, and C. S. Hsu, *Adv. Funct. Mater.* **2012,** 22(8), 1711.
[16] Y. Deng, Y. Chen, X. Zhang, H. Tian, C. Bao, D. Yan, Y. Geng, and F. Wang, *Macromolecules* **2012**, 45(21), 8621.
[17] H. Lai, J. Hong, P. Liu, C. Yuan, Y. Li, and Q. Fang, *RSC Adv.* **2012**, 2(6), 2427.
[18] P. L. T. Boudreault, S. Beaupré, and M. Leclerc, *Polym. Chem*. **2010** 1(2), 127.
[19] P. L. T. Boudreault, S. Wakim, M. L. Tang, Y. Tao, Z. Bao, and M. Leclerc, *J. Mater. Chem.* **2009**, 19(19), 2921.
[20] Z. Deng, L. Chen, F. Wu, and Y. Chen, *J. Phys. Chem. C* **2014**, 118, 6038.
[21] F. Wu, L. Chen, H. Wang, and Y. Chen, *J. Phys. Chem. C* **2013**, 117, 9581.
[22] H. Chen, Y. Gua, X. Sun, D. Gao, Y. Liu, and G. Yu, J, Polym. *Sci. Pol. Chem.* **2013,** 51(10), 2208.
[23] M. J. Sung, S. Yoon, S. K. Kwon, Y. H. Kim, and D. S. Chung, *ACS Appl. Mater. Interfaces* **2016**, 8(45), 31172 ().
[24] S. M. Park, Y. Yoon, C. W. Jeon, H. Kim, M. J. Ko, D. K. Lee, J. Y. Kim, H. J. Son, S. K. Kwon, and Y. H. Kim, *J. Polym. Sci. Pol. Chem.* **2014**, 52(6), 796.
[25] B. Fu, J. Baltazar, Z. Hu, A. T. Chien, S. Kumar, C. L. Henderson, D. M. Collard, and E. Reichmanis, *Chem. Mat.* 2012, 24(21), 4123.
[26] X. Liu, Y. J. Kim, Y. H. Ha, Q. Zhao, C. E. Park, and Y. H. Kim, ACS Appl. Mater. Interfaces 2015, 7(16), 8859.

Research highlight

►Phenanthro[1,10,9,8-c,d,e,f,g]carbazole-based polymer ►Donor-acceptor copolymer ► High solubility for solution process ► Large polycrystalline grains with long range order structure and highly edge-on structure after thermal annealing ► Field effect mobility up to 0.0092 $cm^2 V^{-1} s^{-1}$ after thermal annealing

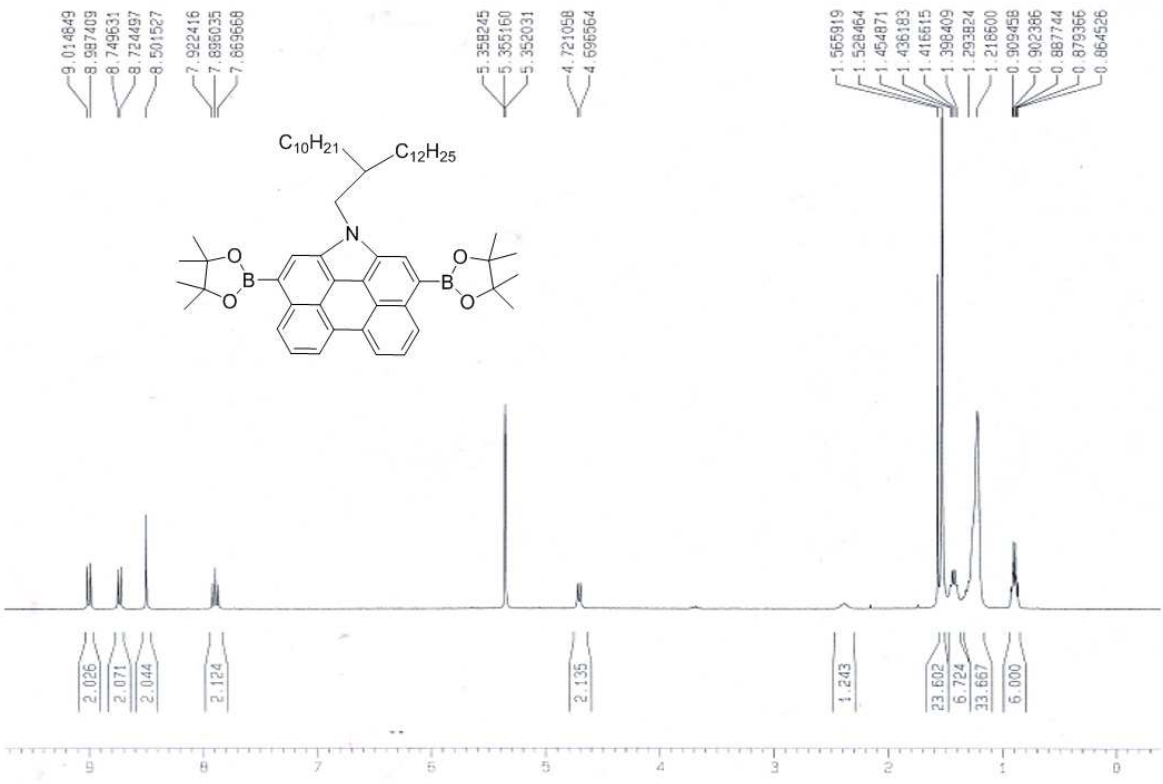
9.014649
8.997409
8.749631
8.724497
8.501527
7.922416
7.896035
7.869668
5.358245
5.355160
5.352031
4.721058
4.696564
1.565919
1.520464
1.454871
1.436183
1.416615
1.398409
1.293824
1.216600
0.909458
0.902386
0.887744
0.879366
0.864526
C10H21
C12H25
N
O
B
O
B
O
O
2.026
2.071
2.044
2.124
2.135
1.243
23.602
6.724
33.667
6.000

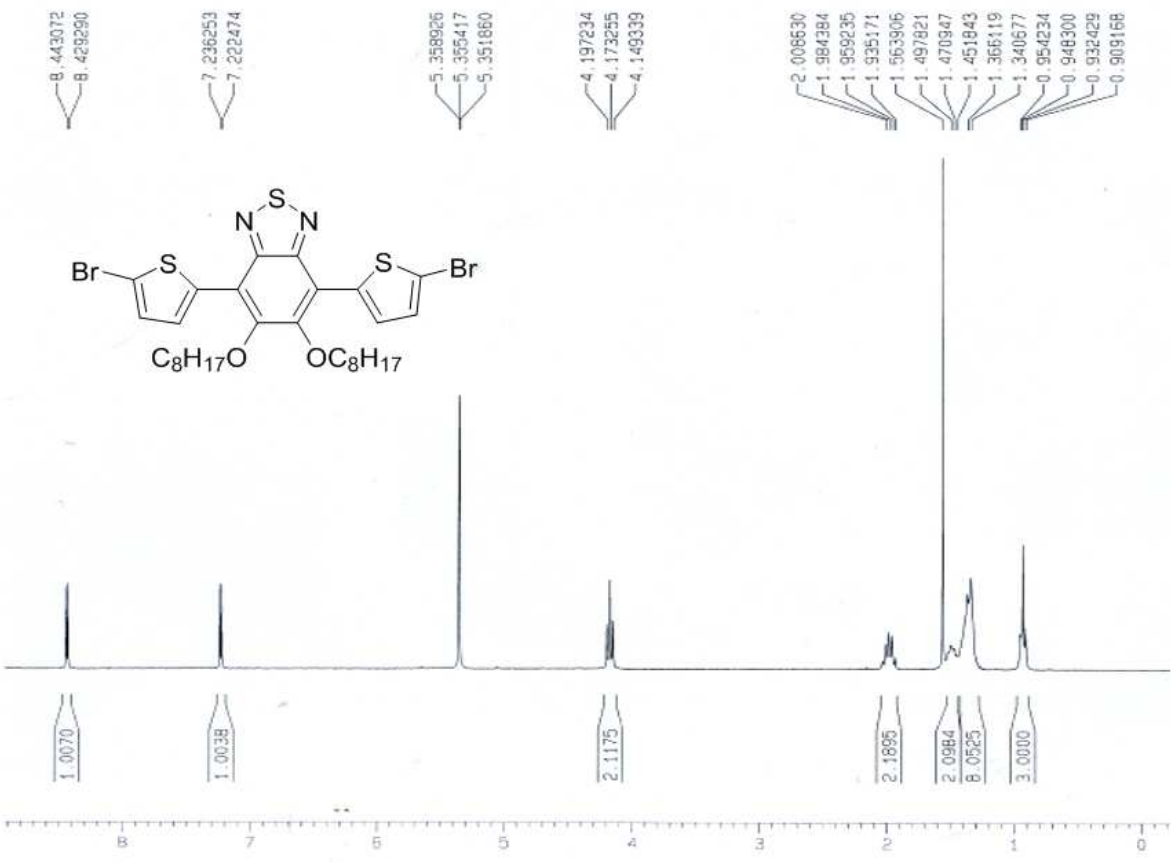
8.443072
8.429290
7.236253
7.222474
5.358926
5.355417
5.351860
4.197234
4.173255
4.149339
2.006630
1.984384
1.959235
1.935171
1.563906
1.497821
1.470347
1.451843
1.366119
1.340677
0.954234
0.948300
0.932429
0.909168
S
N
N
Br
S
S
Br
C8H17O
OC8H17
1.0070
1.0038
2.1175
2.1895
2.0984
8.0525
3.0000

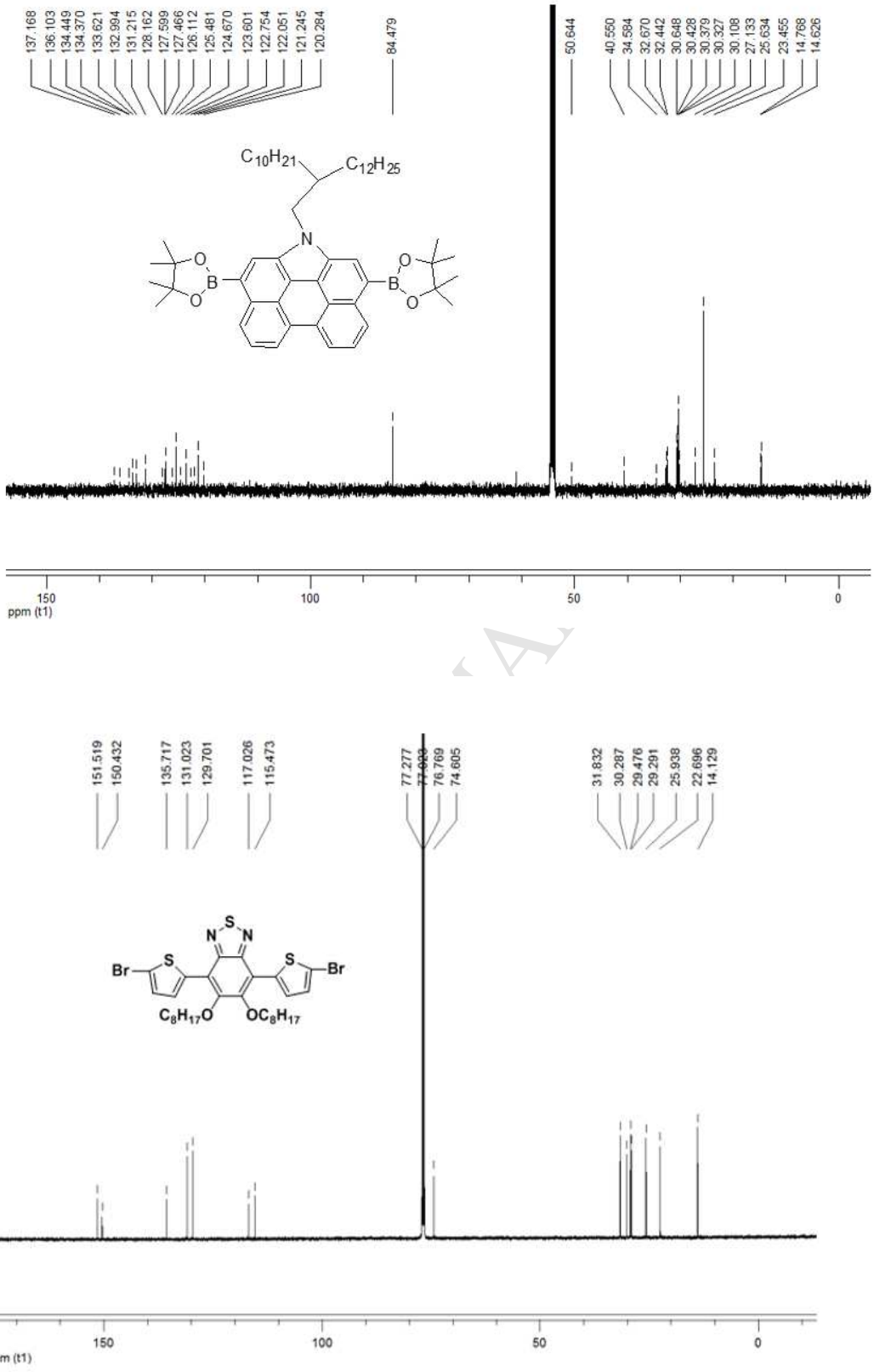

Figure. S1 ^{1}H NMR and ^{13}C NMR spectroscopy of donor and acceptor moiety.

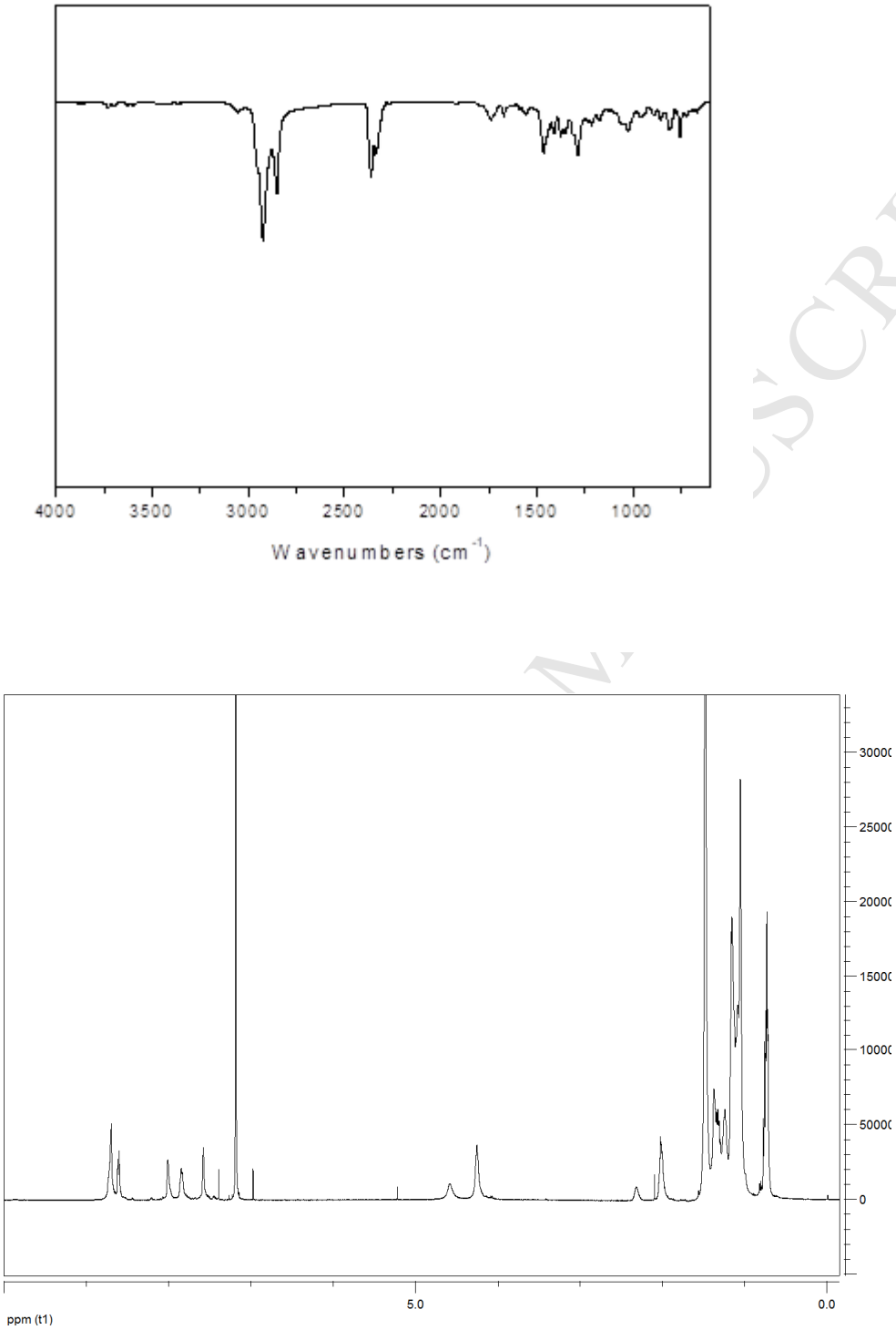

Figure. S1 ^{1}H NMR and IR spectroscopies of polymer.

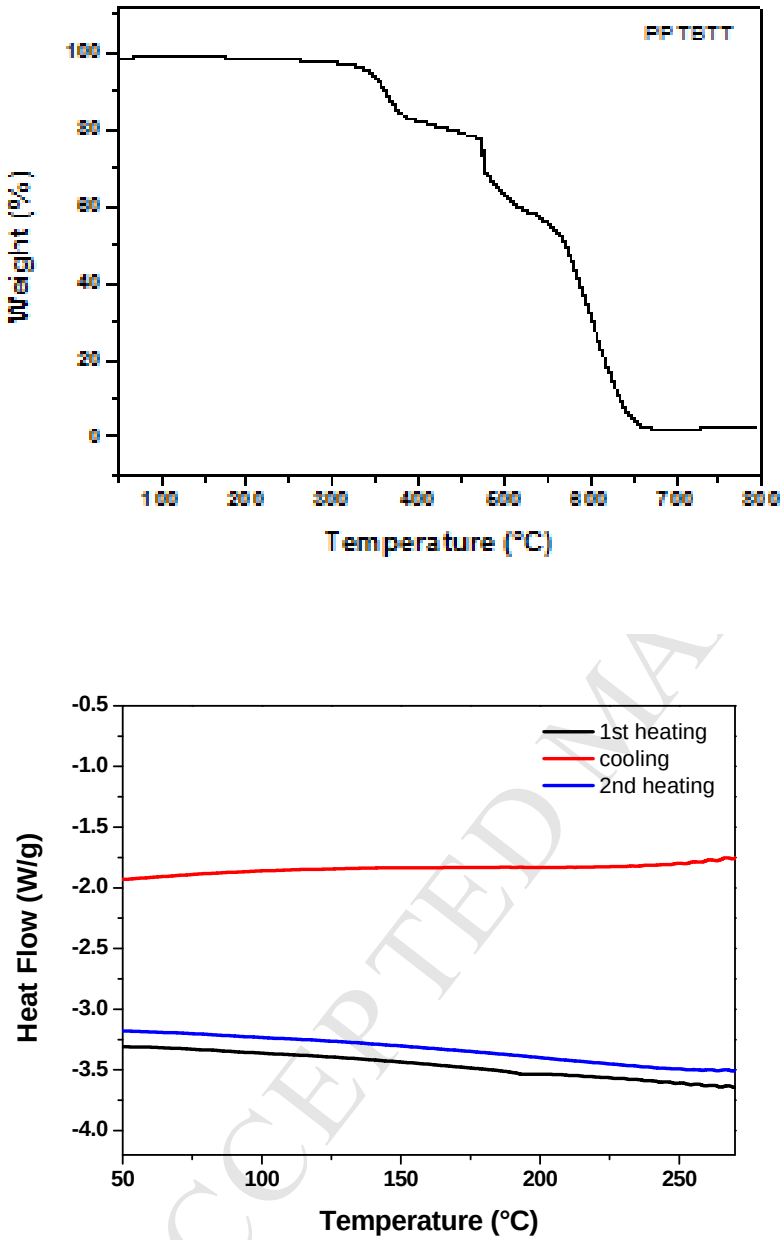

Figure. S3 Thermogravimetric analysis (TGA) and differential scanning calorimetry (DSC) conducted at a heating rate of 10 °C /min.

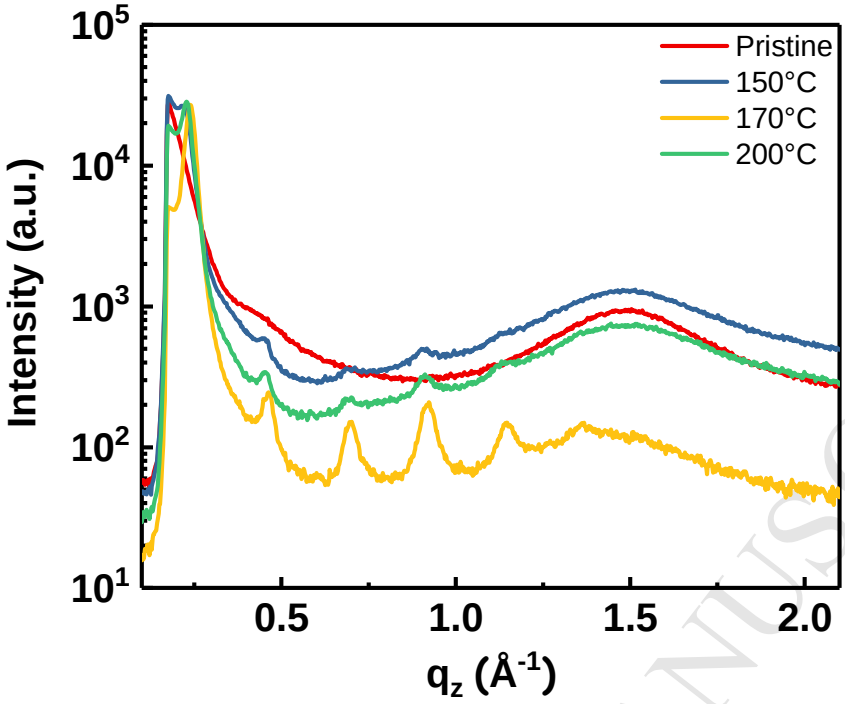

Figure. S4 Out-of-plane line cuts of films annealed at 25 ℃, 150 ℃, 170 ℃, and 200℃.

PPTBTT films annealed at 170℃ showed a long range ordered structure with much more defined out-of-plane Bragg diffraction peaks up to (005).

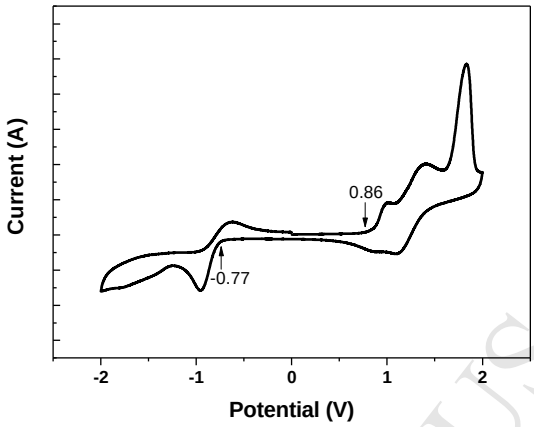

Figure. S5 Cyclic voltammetry (CV) of PPTBTT film in a solution of 0.1 M tetrabutylammonium perchlorate (Bu4NClO4) in acetonitrile at a scan rate of 50 mV/s.

The onset oxidation potential of PPTBTT was 0.86 V, which is calculated to be 5.3 eV for highest occupied molecular orbital (HOMO) level. The calculating the optical bandgap from the UV-vis absorption onset (1.79 eV), the lowest unoccupied molecular orbital (LUMO) level is calculated to be 3.51 eV.